



Structural, AC and DC Electrical Transport Properties of Nano Titania - Polyacrylamide Composite Films

G Veena & Blaise Lobo

Department of Physics, Karnatak University's Karnatak Science College, Dharwad 580 001, Karnataka, India

Received 4 October 2021; accepted 24 February 2022

The microstructural features as well as the AC and DC electrical properties of titanium dioxide (titania or TiO₂) nanoparticle (NP) filled polyacrylamide (PAM) composite films with filler level (FLs) Varied from 0.02 up to 19.5 Wt % were experimentally studied. SEM images revealed that the composite films with FLs equal to 0.02 and 0.40 Wt % (low FLs) showed homogeneous dispersion of spherical TiO₂ NPs, whereas aggregation of the filler was observed at higher FLs. The XRD patterns of these composite films revealed an increase in their amorphousness at low FLs. The activation energy (E_a) determined from Arrhenius equation showed that the composite with FL equal to 0.40 Wt % exhibited the lowest value of E_a (equal to 0.84 eV). Dielectric study revealed that the composite film with FL equal to 0.40 Wt % exhibited the highest value bulk conductivity at room temperature ($4.39 \times 10^{-6} \text{ S m}^{-1}$ at 303 K). Hence, the composite sample with FL 0.40Wt %, along with pure PAM, were subjected to a detailed dielectric study at various fixed temperatures ranging from 303K up to 353K. The composite sample with FL 0.40 Wt % showed a maximum bulk conductivity of $1.12 \times 10^{-4} \text{ S m}^{-1}$ at temperature 353K, while it was $3.45 \times 10^{-8} \text{ S m}^{-1}$ for pure PAM at 303 K.

Keywords: PAM-TiO₂ composite; SEM; FTIR; XRD analysis; AC and DC Electrical properties; Ionic conductivity

1 Introduction

Progress in the field of polymeric composite materials has taken a new lead due to advancements in the preparation and use of nanostructured polymeric materials. The incorporation of an optimum concentration of nanoparticles (NPs) in a polymer matrix makes the nano composite (NC) material possess novel properties^{1,2}. NCs exhibit superior electrical, thermal and mechanical properties when compared with conventional micro-sized or macroscopic filler loaded polymer composites, thereby broadening their area of applications^{3,4}. The synthesis and characterization of composite materials incorporated with different nano-additives have resulted in the fabrication of NC based optoelectronic devices⁵, photovoltaic cells⁶, solar cells⁷, gas sensors⁸, super capacitors⁹ and batteries¹⁰. When fillers like metal oxides are incorporated in a polymeric matrix, there is an increase in the ion transport process, which is caused by reducing the crystalline phase of the host polymeric matrix as well as the formation some favorable ion conductive paths.

Titanium dioxide or titania (TiO₂) is a wide band gap semiconducting metal oxide which is well known

for its good electronic properties, thermal stability and good photo-catalytic properties. TiO₂ based polymer electrolytes have been studied for various applications like gas sensors¹¹, photo catalysts¹² and dye sensitized solar cells¹³. The host polymeric material, PAM (or poly(2-propanamide)) is an eco-friendly, biodegradable polymer. PAM has been widely studied due to its affinity for water and because of its amorphous microstructure, both of which have been exploited by various researchers, in order to use it for the fabrication of a stretchable and transparent electrolyte for zinc batteries¹⁴. PAM based polymer composites has been extensively studied by various researchers^{15,16}. TiO₂ NPs are of special interest for use as a nano-filler, because they are inexpensive and non-toxic; their electron rich nature improves the electrical conductivity of the composite in which they are incorporated by interacting with carbonyl groups present in the polymer.

In this paper, TiO₂ NPs were loaded in PAM and the structural features as well as electrical transport properties of the resultant composite have been experimentally investigated. The interaction of TiO₂ NPs with PAM results in structural modifications of the host polymeric matrix (PAM) due to the formation of charge transfer complexes (CTCs), thereby creating

*Corresponding author: (E-mail: blaise.loba@gmail.com)

favorable conduction paths for the mobility of charge carriers in the composite material. As a result of this, there is an enhancement in the amorphousness and ionic conductivity of the composite material. These properties of the titania filled PAM composite can be further enhanced by adopting methods such as irradiation, iodine sorption or by incorporating another filler in the form of a salt, which can provide additional charge carriers and makes the material more suitable for energy storage applications such as fuel cell, battery and solar cells. However, this study is important to understand the effect of TiO₂ NP alone on the various properties of PAM matrix and acts as a basic control study to further exploit the properties of this composite material.

2. Materials and Methods

2.1 Sample preparation

Solution casting technique was used to obtain the composite films of PAM and TiO₂ NP filled PAM with FL ranging from 0.0 to 19.5 Wt %. PAM with molecular mass 5,000,000 g/mol was procured from Himedia laboratories Pvt. Ltd., Mumbai, India. Spherical NPs of TiO₂, whose average particle size is 65 nm were obtained from Ultra Nanotech Private Limited, Bengaluru, India. Aqueous solution of PAM was prepared by dissolving 0.50 grams of PAM in 200 ml of double distilled water. In order to prepare the PAM-TiO₂ composite, the required weighed amount of TiO₂ NPs was dispersed in distilled water using an ultrasonicator; this dispersion (mixture) was then transferred to aqueous PAM solution (taken in a glass beaker) in different volumes. The mixture, in each case, was poured into a clean glass petridish and then kept in an air cooled, temperature controlled oven maintained at 50°C for several days in order to dry the films by solvent evaporation method. After drying, the films were peeled from the glass petridishes, properly labeled and stored in a desiccator.

2.2 Methods

X-Ray diffraction (XRD) scans of pure and TiO₂ NP filled PAM composite were obtained at room temperature using Rigaku Miniflex 600 X-ray diffractometer, with Cu K_α X-rays of wavelength 1.5406 Å as the incident radiation. SEM images were obtained using Nova NanoSEM, a field emission scanning electron microscope (FE-SEM). Temperature dependent DC electrical measurements for pure PAM and TiO₂ NP filled PAM composite

were carried out using a research grade two probe set up which consisted of a PID controlled oven (model: PID-200), high voltage power supply (model: EHT-11) and a digital picoammeter (model: DPM-111) (purchased from SES Instruments Pvt. Ltd. Roorkee, India).

Dielectric measurements were carried out by using a precision LCR meter, GWINSTEK LCR821, a research grade apparatus from Good Will Instruments Co. Ltd., Taiwan. The dielectric studies at fixed temperatures were performed by varying the frequency from 12 Hz up to 200 kHz, at different set temperatures (using a PID controlled furnace, with an accuracy of 0.1 °C). The values of impedance (Z) and phase angle (θ) between the applied alternating field and the generated current were experimentally determined at different frequencies of applied AC signal, and at different sample temperatures. For precise measurements while using the LCR meter, the readings which are taken in the “slow” mode of measurement.

3 Results and discussion

3.1 X-ray diffraction

XRD scans were obtained in the scattering angle (2θ) range varying from 10° up to 80°. In the case of pure TiO₂ NPs, the characteristic diffraction peaks (corresponding to the anatase phase of TiO₂) were obtained at 2θ = 24.34°, 37.90°, 47.96°, 53.9°, 55.06°, 62.7° and 68.83°, corresponding to crystal planes with Miller indices (101), (004), (200), (105), (211), (204) and (114), respectively^{17, 18}. These values match with the JCPDS file number 21-1272, which corresponds to anatase TiO₂. A broad band at 2θ equal to 23° for pure PAM manifests the short range (local) order, and therefore reflects the extent of the amorphous nature of PAM. Fig. 1 shows the XRD scans of TiO₂ NPs, pure PAM and TiO₂ filled PAM composite films. Degree of crystallinity (X_C) of the semi-crystalline composite films was estimated by considering the contributions of both amorphous and crystalline regions of the sample by utilizing Equation 1, which follows.

$$X_C = \frac{A_C}{A_C + A_A} \quad \dots (1)$$

In Equation 1, A_C and A_A are the areas under the crystalline peaks and the amorphous profile, respectively.

The values of X_C listed in Table 1 reveals that X_C has decreased for titania NP filled PAM at lower FLs,

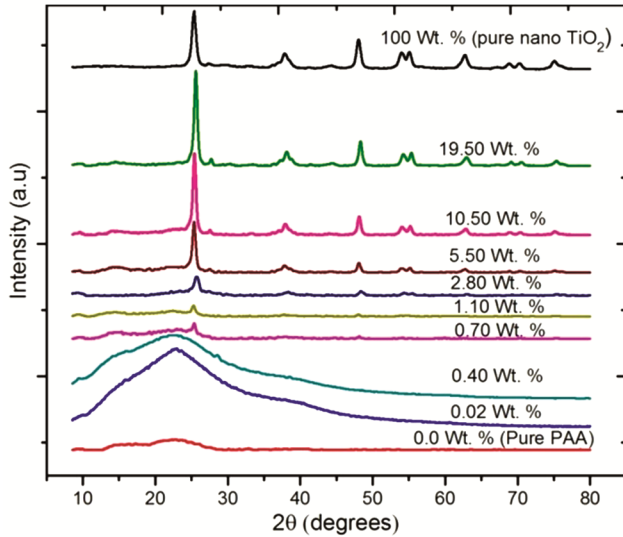


Fig. 1 — XRD scans of TiO₂ NPs, pure PAM and TiO₂ NP filled PAM films.

Table 1 — Degree of crystallinity (X_C) calculated from XRD scans, of pure PAM and TiO₂ NP filled PAM composite films

FL (Wt %)	0.00	0.02	0.40	0.70	2.80	5.50	10.5	19.5
X_C (%)	8.50	5.80	5.20	6.10	9.49	9.40	11.90	17.40

when compared to pure PAM but beyond a FL of 1.10 Wt%, the value of X_C has increased. It can be seen that, at lower FLs (at 0.02 and 0.40 Wt %), the crystalline peaks of TiO₂ are not visible, which implies a uniform dispersion of titania NPs in PAM matrix (also see the SEM images). For composite films with FLs 0.70 and 1.10 Wt%, the value of X_C has slightly increased, but it is lower than that of pure PAM as the aggregation of titania NPs has just begun at these moderate FLs. The value of X_C in the case of TiO₂ NP filled PAM composite samples has decreased because the incorporated TiO₂ NPs interacts with the polymeric host matrix leading to the destruction of even the short range ordered arrangements of polymer chains. This is manifested in the powder XRD scans of these composite samples as a broadening of the amorphous halo for the composite samples at lower FLs. For films with FL of 2.80 Wt % and above, sharp crystalline peaks with increasing intensities (with increase in FL of titania in the prepared composite) are observed in the XRD scans of the corresponding titania NP filled PAM composite. This can be attributed to the filling up of free volume holes (dynamic open spaces in the amorphous regions of the polymeric host material) by aggregates of TiO₂ NPs; obviously, as evidenced from the XRD scans, this happens in the composite films at higher FLs and results in the increase in value

of X_C with further increase in FL. The variation in the value of X_C of the composite sample with increase in FL mainly depends on the nature of polymer host, the nature of the added NPs and the method employed for preparation of the composite material. Literature reveals an enhancement in amorphousness of the polymeric composite due the addition of TiO₂ as the nano filler¹⁹.

The interaction of TiO₂ NPs with PAM takes place by the formation of CTCs, caused by inter-molecular and intra-molecular hydrogen bonding^{20, 21} (FT-IR analysis of this composite can be seen in the supplementary file). The mobility of cationic and anionic charge carriers in the polymer matrix results in improved ionic conductivity of these composite materials. Segmental motion of the polymeric chains in the amorphous phase of the polymeric material is responsible for a further enhancement in ionic conductivity of the composite material. Also, the CTCs create favorable conduction paths for the mobility of charge carriers in the composite material. Therefore, an increase in amorphous phase of the polymer electrolyte results in an enhancement of its ionic conductivity. At low FLs of TiO₂ NPs in PAM, there is an increase in the amorphousness of the resulting composite film and so there will be an increase in its ionic conductivity. But, on successive addition of semiconducting TiO₂ NPs, there is aggregation of these NPs and this adversely affects the ionic conductivity of the resultant composite film. The reduction in free volume in the composite material at higher FLs, due to filler aggregation, hampers the movement of ions in it.

The area under crystalline peaks in the XRD scans and full width at half maximum (β) of the crystalline peaks were determined in order to calculate some of the structural parameters. In order to calculate the average crystallite size (P), the following equation is used.

$$P = \frac{k\lambda}{\beta \cos\theta} \quad \dots (2)$$

In Equation 2, P is the average crystallite size, k is a constant which is equal to 0.9 and λ is the wavelength of incident Cu K α - X-rays, which is equal to 1.5406 Å. The values of P are listed in Table 2, which suggest that the crystallite size is in the nano-meter scale. It can be observed that there is an increase in crystallite size for the composite samples at higher FLs (and at higher angles of diffraction) is attributed to the aggregation of titania NPs in the host PAM matrix. Average separation between crystallites is given by Equation 3, which follows.

Table 2 — Structural parameters calculated from XRD scans of pure PAM and TiO₂ NP filled PAM composite films

FL (Wt %)	2θ (degree)	P (nm)	R (Å)	d (Å)	δ (x 10 ¹⁸ m ⁻²)	ε (x 10 ⁻²)	<N> (x10 ²² m ⁻²)
100 (TiO ₂ NP)	25.30	13.1	4.39	3.5	0.05	3.13	-
0.70	25.33	13.9	4.38	3.51	0.05	1.09	0.002
1.10	25.27	13.49	4.40	3.52	0.005	1.14	0.001
2.80	25.69	13.34	4.32	3.56	0.01	1.37	6.32
5.50	25.36	17.69	4.38	3.50	0.031	0.89	0.018
10.50	25.40	15.59	4.37	3.50	0.04	1.01	0.020
19.50	25.58	13.44	4.35	3.47	0.065	1.12	0.004

$$R = \frac{5\lambda}{8 \sin\theta} \quad \dots (3)$$

The inter-planar spacing (or *d*- spacing) is obtained from Bragg's equation, which for first order is given as follows,

$$d = \frac{\lambda}{2 \sin\theta} \quad \dots (4)$$

Interplanar spacing (*d*) of a material is the constant distance between the constituent atoms in different planes in the crystal structure of the material. It is a characteristic property of the material. Table 2 lists the calculated values of *d* for crystalline peaks in the sample. The values of *d* for characteristic diffraction peaks corresponding to the anatase phase of TiO₂ in titania filled PAM composites are in good agreement with the values reported in the literature for anatase TiO₂ NP²². It is to be noted that the values of *d* spacing for a particular peak in samples with different FLs are comparable (to each other).

Micro-strain or lattice strain values are calculated using Equation 5. Micro-strains occur in the crystal as a result of defects in the material, which includes dislocation and twinning, which is responsible for the broadening of XRD peaks.

$$\epsilon = \frac{\beta \cot\theta}{4} \quad \dots (5)$$

Dislocation refers to the irregular arrangements or deformations appearing in the crystallographic structure of the material. Dislocation density (δ) is a measure of dislocation length per unit volume of the material. Incorporation of TiO₂ NPs into the PAM creates dislocations or defects in the few crystalline regions of the composite system, which causes changes in optical, thermal and electrical properties of the host polymeric material. Dislocation density (δ) is given by Equation 6, which follows

$$\delta = \frac{1}{P^2} \quad \dots (6)$$

Table 2 list the value of micro-strain and dislocation density of pure PAA and TiO₂ NP filled

PAM. It can be seen that a for all the samples, the values of micro-strain and dislocation density are greater at low angles of diffraction, while these values are found to be less at higher angles of diffraction. In case of TiO₂ NPs filled PAM samples, the lattice strain may arise due to the excess volume of grain boundaries due to dislocations. Lattice strain is caused as a result of displacement of atoms with respect to their reference lattice strain. The occurrence of micro strain can be related to lattice misfit.

Average number of crystalline unit cells per unit area (<N>) is given by Equation 7, which follows.

$$\langle N \rangle = \frac{t}{p^3} \quad \dots (7)$$

Table 2 lists the values of various structural parameters for major crystalline peak for the composite sample.

3.2 SEM Analysis

The incorporation of TiO₂ NPs in PAM matrix affects the morphology of PAM, which has been visualized using SEM (see Fig. 2, also shows the particle size distribution (PSD) of the titania NPs embedded in PAM, for the composite samples at low FLs of 0.02 and 0.40 Wt%)

From the SEM images of pure PAM, a plane homogeneous surface is observed, implying that there are no additional micro-structural or nano-structural features, as expected for the case of pure PAM. For composite films with lower FLs of titania, such as 0.02 and 0.40 Wt %, a good dispersion of TiO₂ NPs showing their bead like structures dispersed homogeneously in the host polymeric matrix (PAM) is observed. However, the aggregation of TiO₂ NPs occurs at higher FLs. This aggregation of NPs is accompanied by an increase in the degree of crystallinity of the composite, and it is manifested in the form of crystalline peaks corresponding to nano- TiO₂ in the XRD scans. At the moderate FL of 0.70 Wt%, the NPs have started to form clusters which can be seen the micrographs. At still higher FLs, from 2.8 Wt % up to 19.5 Wt %, agglomeration of NPs in the host material takes place to

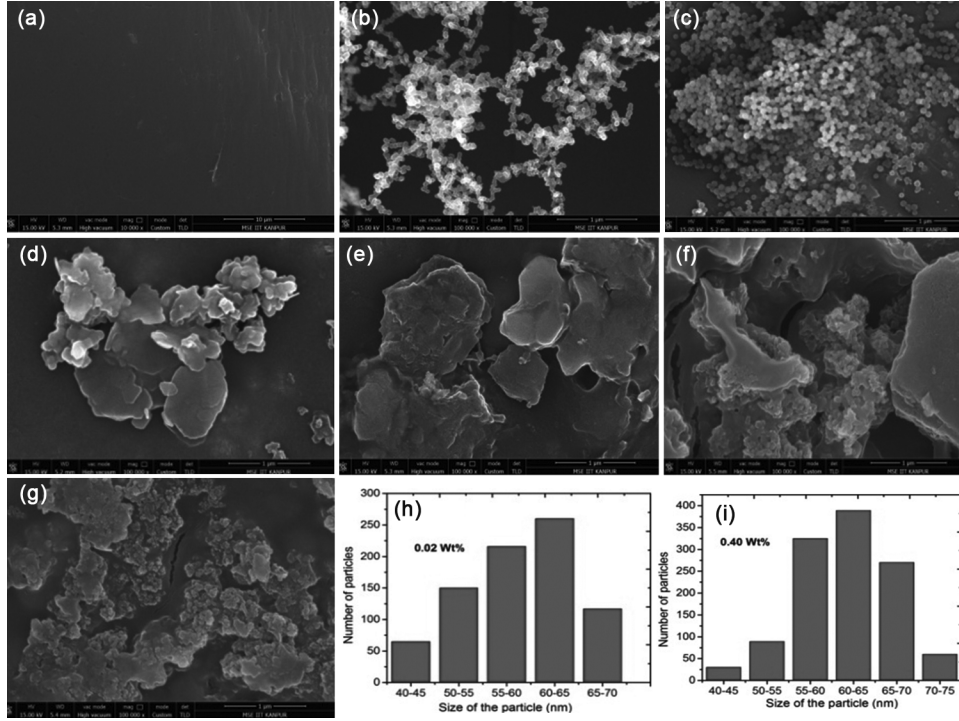


Fig. 2 — SEM images of TiO₂ NP filled PAM composite films with FLs equal to (a) 0.0 Wt %, (b) 0.02 Wt %, (c) 0.40 Wt %, (d) 0.70 Wt %, (e) 2.8 Wt %, (f) 5.5 Wt % and (g) 19.5 Wt %. Particle size distribution is presented in (h) 0.02 and (i) 0.40 Wt %.

a much larger extent, which is accompanied by an increase in the value of X_C and the emergence of sharp crystalline peaks of TiO₂ NPs in the XRD scans, as well as a decrease in electrical conductivity of these composite films (which has been discussed later, in detail). The dispersion of TiO₂ NPs in PAM matrix has resulted in modifications in the microstructure of the resulting composite material. Interaction between TiO₂ NPs and the polymer matrix provides an additional mechanism of ionic conductivity, which is enhanced along the NP-polymer interface. Therefore, the highest ionic conductivity of the titania filled PAM composite is achieved by the addition of 0.40 wt % of TiO₂ (where a good dispersion of NPs is observed) due to increase in the mobility of charge carriers.

The addition of TiO₂ NPs beyond 2.8 wt % makes the surface morphology rough, due to aggregation of NPs, and this composite has a lower value of ionic conductivity (discussed in a later section (section 3.3) of this paper). It can be seen from the SEM images of the composite samples at higher FLs that the cluster or aggregates of the NP are not uniformly distributed on the surface of the sample.

3.3 DC electrical measurements

The effect of incorporating TiO₂ NPs on the electrical conductivity of PAM matrix was

systematically studied by using DC electrical measurements. The sample was sandwiched between two aluminum electrodes and the current was monitored as a function of temperature, after the application of a fixed stable DC voltage across the composite sample. Proper contact between the composite sample and the electrode was done by pasting silver on the surface of the sample, on either side. Activation energy for the mobility of charge carriers due thermal activation was determined by using the Arrhenius equation.

$$\sigma = \sigma_0 \exp\left(\frac{-E_a}{k_B T}\right) \quad \dots (8)$$

$$E_a = -m \times k_B \quad \dots (9)$$

$$\text{Where, } m = \frac{d(\ln\sigma)}{d(1/T)}$$

In Equation 8, σ is the electrical conductivity, σ_0 is the pre-exponential factor, k_B is the Boltzmann constant and E_a represents the activation energy. Fig. 3 illustrates the temperature dependence of DC conductivity of PAM and TiO₂ filled PAM composites, in the temperature range varying from 303K to 333K.

The plot of $\ln\sigma$ versus reciprocal absolute temperature has a straight line nature, indicating that the electrical conductivity is thermally activated, with

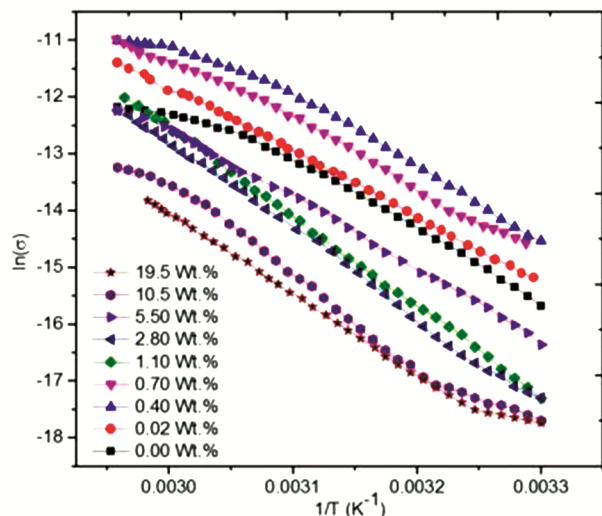


Fig. 3 — Plot of the logarithm of the electrical conductivity versus reciprocal of the absolute temperature ($1/T$), for pure PAM and TiO_2 filled PAM composites.

Table 3 — Values of activation energy (E_a) for pure PAM and TiO_2 NP filled PAM composite

FL (Wt %)	E_a (eV) (DC electrical)	t_{ion}	t_e
0.00	1.16	0.992	0.008
0.02	0.96	-	-
0.40	0.84	0.982	0.018
0.70	1.06	0.980	0.020
1.10	1.11	0.983	0.017
2.80	1.09	0.986	0.014
5.50	1.20	-	-
10.5	1.37	0.985	0.015
19.5	1.54	0.983	0.017

a single value of E_a . The slope of the plot of $\ln \sigma$ versus reciprocal absolute temperature was used to calculate the values of E_a (see Table 3) for PAM and TiO_2 filled PAM composite. It was noted that the value of E_a for PAM lies in between the corresponding values for the composite at lower FLs and higher FLs of TiO_2 filled PAM composite. The conductivity behavior can be explained by using the hopping charge mechanism. The increase in electrical conductivity with temperature implies that the process is a thermally activated one. With an increase in temperature, the segmental motion of polymeric chains is enhanced and the mobility of charge carriers is also increased. A decrease in value of E_a is observed for the composite sample at low FLs; E_a reduces to a lowest value of 0.84 eV for the composite sample with FL 0.40 Wt% from a higher value of 1.16 eV, which is observed for pure PAM. This is due to the increase in number of charge carriers in the composite sample provided by the incorporated NPs.

At low FLs, the addition of TiO_2 NPs has aided the ion transportation in the composite by reducing the crystalline phase of the host polymer (as evidenced from the XRD scans). The titania NPs which have been incorporated in the host polymer reduces the barrier height of the trapping sites by forming CTCs, there by forming favorable ion conductive paths. The “electron pair” acceptor group of TiO_2 interacts with oxygen in the polymer to form a CTC. These interactions create new pathways for the hopping of charge carriers across the localized sites, by transferring the charge from one CTC to another. On further loading of the filler, there is an increase in the value of E_a for the titania NP filled PAM composite films with FLs 0.70 Wt % and 2.8 Wt. %, which can be attributed to the fact that the agglomeration of TiO_2 NPs occurs in these composites; hence, the E_g values for composites at these FLs are less than that of the pure sample. But for higher FLs, say from 5.5 Wt % up to 19.5 Wt %, the aggregation of titania NPs incorporated in PAM takes place to a greater extent, which results in a larger separation between conducting regions, and this leads to hopping of charge carriers to a lesser extent. At very high FLs, beyond 2.80 Wt %, the agglomeration of titania NPs in the host (PAM) matrix leads to a significant decrease in the segmental mobility of polymeric chains, which results in the composite samples having a lower value of electrical conductivity.

3.4 Time dependent study

Polymeric materials are mainly ionic conductors. Even in the case of PAM and TiO_2 NP filled PAM composites, when a potential difference (or voltage) is applied across the composite sample, the main contribution to the total electrical current is from ions, whereas the electronic contribution to the total current is low. Transport number denotes the fraction of current carried by mobile ions or electrons, in terms of total current I_T . Transference number of ions (t_i) and electrons (t_e)²³ were determined using Wagner’s polarization technique²⁴, which is also known as the DC polarization technique. In this method, the composite sample (film) was sandwiched between two electrodes, among which one was a blocking electrode (graphite electrode). To enable this, the sample was coated with graphite paste on one side of the sample and silver paste on the other. The evolution of DC electric current was monitored as a function of time, under a steady DC potential of 1.1V (step voltage), which is below the decomposition potential of the sample.

Figure 4 depicts the nature of variation of the DC polarization current versus time (time evolution plot) for PAM and TiO₂ NP filled PAM composite samples, respectively. It can be seen from Fig. 4 that the current drops from a certain value (say, $I_T = I_{i+e}$) to reach a lower steady state value (denoted by I_{el}) after a long time. Initial current depends on the applied voltage, and is the sum of the contributions (to the current) from both ions and electrons ($I_T = I_{i+e} = I_{ion} + I_{el}$). Later, there is formation of a passivation layer of ions at the interface of the blocking electrode and the electrolyte interface, due to which, the interfacial resistance increases²⁵. Consequently, the ionic current is blocked. Now, the charge transport occurs only by electron motion. Therefore, the final current is only due to transport of electrons. Transference number for electrons (t_e) is calculated from Equation 10, which follows.

$$t_e = \frac{I_{el}}{I_T} \quad \dots (10)$$

In Equation 10, I_{el} is the current due to electrons or the final current and I_T is the initial total current (due to both electrons and ions).

Transference number for ions (t_{ion}) is calculated using Equation 11, which follows.

$$t_{ion} = 1 - t_e \quad \dots (11)$$

The values for ionic and electronic transference numbers are listed in Table 3 for different FLs of TiO₂ NPs in PAM. Although ions are the major charge carriers in the titania NP filled PAM composite material, it can be seen that the incorporation of these semiconducting NPs (NPs of TiO₂) in the PAM matrix

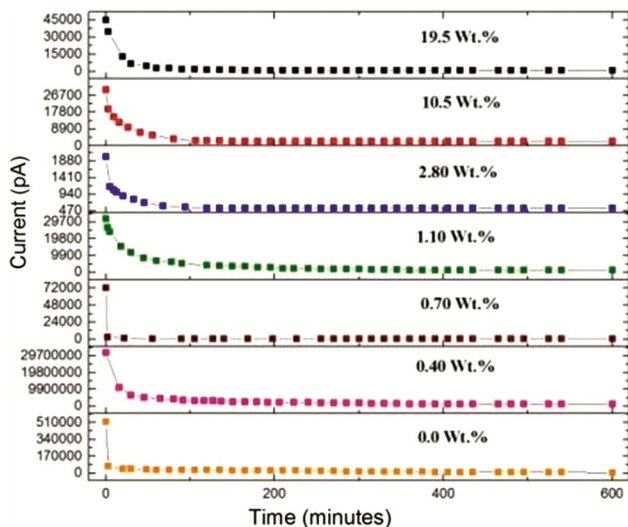


Fig. 4 —DC polarization current versus time plot for PAM film and TiO₂ NP filled PAM composite samples.

has resulted in a significant increase in the electronic transference number of the TiO₂ filled PAM composite.

3.5 AC Impedance study

The experimental determination of AC conductivity is an effective method to study the ionic conductivity behavior of polymer composite films. Unlike DC electrical measurements, the accumulation of charge carriers at the interface between the sample and electrode is avoided by using the AC measurement technique. This technique involves the measurement of impedance (Z) and phase angle (θ), at various frequencies of an input AC signal and at different sample temperatures. Impedance analysis accounts for various relaxation processes which take place in bulk of the electrolyte, grain boundaries and electrode-electrolyte interfaces of the composite film.

3.5.1 Frequency dependent AC Impedance study

The impedance measurements were carried out by sandwiching the composite film between metal electrodes in a two probe set up; the sample films which were cut to proper size were sandwiched between a steel electrode on one side of the sample and an aluminum (Al) electrode on the other side. Data in the form of experimental values of Z and θ for different set frequencies varying from 12 Hz to 200 kHz were obtained by using a precision LCR meter interfaced to a personal computer. The Z and θ values for pure PAM and TiO₂ NP filled PAM composite films, for FLs varying from 0.0 Wt % up to 19.50 Wt%, were analyzed to obtain a Cole-Cole plot (Nyquist plot) as shown in Fig. 5. The nature of Cole-Cole plot for pure PAM is a single semicircle

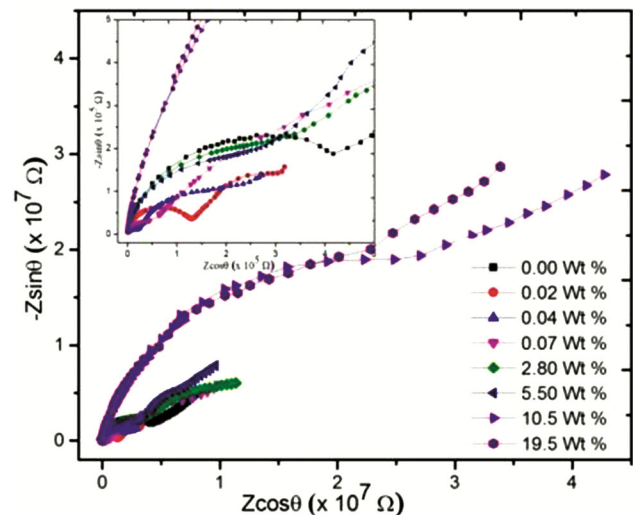


Fig. 5 — Cole-Cole plot for PAM and TiO₂ NP filled PAM polymer composite films.

followed by a spike, while for TiO₂ NP filled PAM, the nature of Cole-Cole plot is a double semicircle, followed by a spike. The first semicircle in the higher frequency region signifies the ionic conduction, due to mobility of charge carriers (ions) in the bulk of the polymer composite, while the semicircle at lower frequencies is due to the contribution to ionic conductivity from the grain boundaries. The spike following the semicircle is due to the electrode-electrolyte interface. In the case of an ideal homogeneous interface, the spike is expected to be inclined at an angle of 90° to Z' axis (real component of the impedance) or parallel to Z'' axis (imaginary component of the impedance). The electrical conductivity is due to ion mobility in the bulk of the sample. The bulk conductivity (σ_b) for pure PAM and TiO₂ NP filled PAM composite films was determined by using the following formula.

$$\sigma_b = \frac{d}{R_b \times A} \quad \dots (12)$$

In equation (12), the parameters d , A and R_b represents the thickness of the composite film, area of the sample sandwiched between the electrodes and bulk resistance of the material, respectively. The value of R_b is obtained by extrapolating (and thereby intersecting) the semicircle obtained by fitting the points in the Cole-Cole plot, and extrapolating the fitted curve to the real axis.

The values of σ_b for pure and TiO₂ NP filled PAM composite films (which have been listed in Table 4) reveals that the incorporation of TiO₂ NPs into the PAM matrix has greatly affected the ionic conductivity of the polymer electrolyte. Initial increase in the value of σ_b indicates that the incorporation of TiO₂ NPs in PAM makes more number of charge carriers or ions available for conduction; hence, the ionic conductivity is enhanced²⁶. But, on further loading of TiO₂ NPs in PAM, the aggregation of these NPs occur in the host polymeric material, which reduces the segmental motion of the polymeric chains as well as impedes the motion of ions, thus adversely affecting the ionic conductivity of the composite film. Hence, the ionic conductivity has decreased for the composite samples at a moderate FL of 0.70 Wt %, whereas at a higher FL of 19.5 Wt %, the value of σ_b has decreased to a

value of $1.01 \times 10^{-8} \text{ Sm}^{-1}$, which is less than the ionic conductivity of pure PAM ($3.45 \times 10^{-8} \text{ Sm}^{-1}$).

Polymer electrolytes follow non - Debye nature of AC conductivity. Cole modified the Debye equation for complex permittivity in order to account for various relaxation processes occurring in the polymer electrolyte; the modified equation is as follows.

$$\epsilon^* - \epsilon_\infty = \frac{\epsilon_0 - \epsilon_\infty}{1 + (i\omega\tau)^{1-\alpha}} \quad \dots (13)$$

In Equation (13), α is an empirical parameter. The composite film sandwiched between two electrodes acts as a parallel plate capacitor. The values of dielectric constant (ϵ') and dielectric loss (ϵ'') are calculated by using Equations (14) and (15), which follow.

$$\epsilon' = \frac{Cd}{\epsilon_0 A} \quad \dots (14)$$

$$\epsilon'' = \epsilon' \tan\delta \quad \dots (15)$$

In equation (14) and equation (15), C is the capacitance of the sample, ϵ_0 is the permittivity of free space and $\tan\delta$ is the loss tangent.

3.5.2 Temperature dependent study

Among all the TiO₂ NP filled samples, the composite sample of the 0.40 Wt % TiO₂ NP filled PAM sample exhibited the maximum value of bulk conductivity and dielectric constant at room temperature. This is due to the uniform dispersion of titania NPs in the polymer matrix. Thus, the titania NP filled PAM composite films with FL 0.0 Wt % and 0.40 Wt % were chosen for a detailed AC impedance study at various fixed temperatures. Impedance data were extracted for a range of frequencies at various fixed temperatures, ranging from 303K up to 353K. Fig. 6(a) and Fig. 6(b) represent the Cole-Cole plot for PAM and 0.40 Wt % TiO₂ NP filled PAM (maintained at various fixed temperatures), respectively. We see that the diameter of the tilted semicircle for both PAM and 0.40 Wt % filled PAM decreases with an increase in the set sample temperature, which implies that there is an increase in the bulk ionic conductivity with an increase in the temperature, indicating that the process is a thermally activated one. With an increase in sample temperature, the segmental mobility of polymer (PAM) chains increases, which enable the free motion of charge carriers in the presence of the applied field;

Table 4 — Values of σ_b for PAM and TiO₂ NP filled PAM polymer composite films, at room temperature

FL (Wt %)	0.00	0.02	0.4	0.7	2.80	5.50	10.50	19.50
$\sigma_b (\text{Sm}^{-1})$	3.45×10^{-8}	1.45×10^{-7}	4.39×10^{-6}	1.8×10^{-7}	1.48×10^{-7}	2.89×10^{-8}	1.92×10^{-8}	1.01×10^{-8}

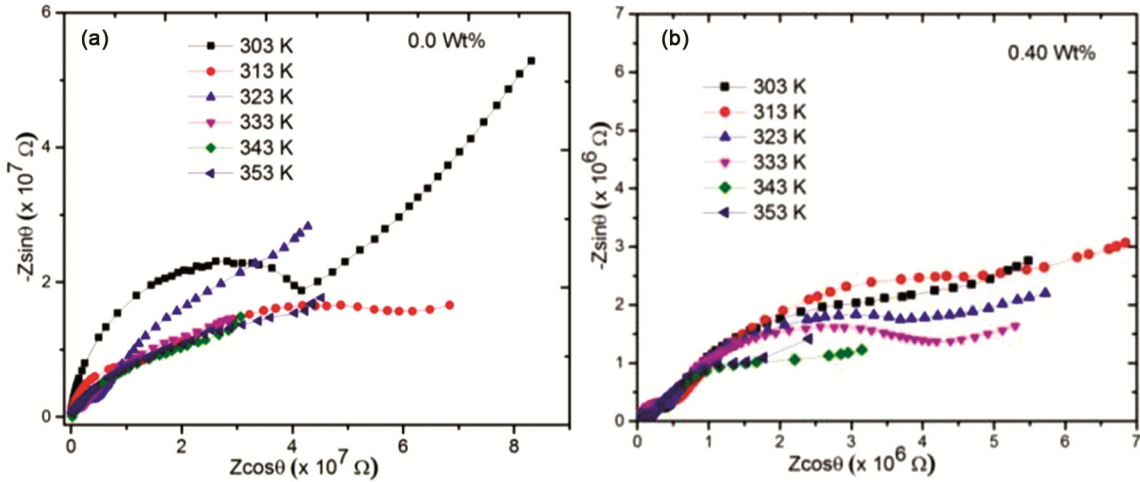


Fig. 6 — Cole-Cole plot for (a) PAM and (b) 0.4 Wt % TiO₂ NP filled PAM, at various set temperatures.

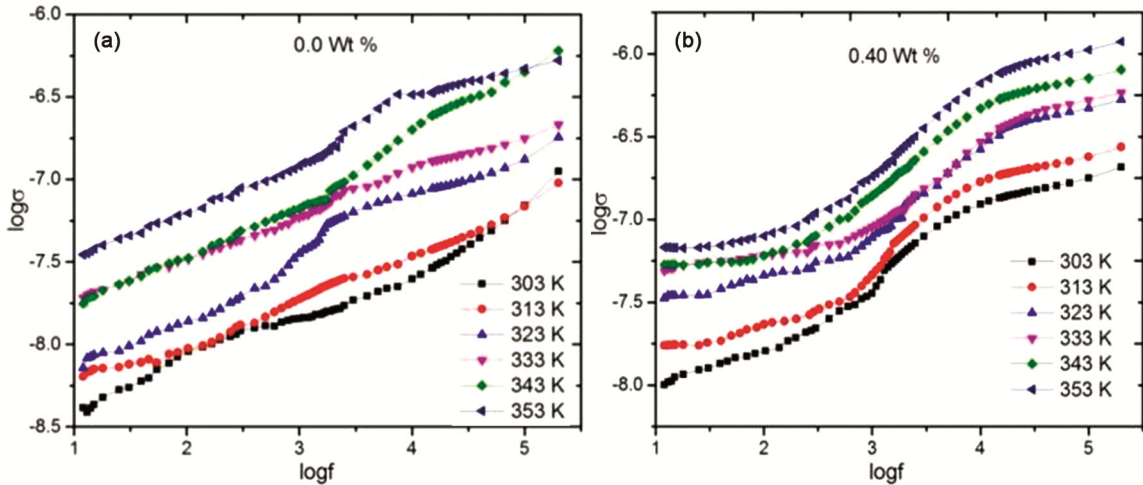


Fig. 7 — Frequency dependence of AC conductivity (σ) for (a) PAM and (b) 0.40 Wt % filled TiO₂ NP filled PAM composite at different temperatures.

therefore, the AC conductivity of the sample is enhanced with an increase in its temperature. The values of bulk conductivity for 0.0 and 0.40 Wt % composite with respect to temperature are listed in Table 5.

Application of AC field increases the conductivity of TiO₂ NP filled PAM composite films due to the enhanced flexibility. AC conductivity of the sample is calculated by using the following equation.

$$\sigma = \omega \epsilon_0 \epsilon'' \quad \dots (16)$$

Fig. 7 shows the plot of $\log\sigma$ versus $\log f$ at various set temperatures, for pure (0.0 Wt %) and 0.40 Wt % TiO₂ NP filled composite sample. We see that the value of $\log\sigma$ increases with increase in frequency (f). In case of pure PAM, the flexibility of bonds is caused by the rotation of functional groups (present in

Table 5 — Values of s_1 , σ_b , s and W_h for pure PAM and TiO₂ NP filled PAM composite film with FL 0.4 Wt%, at different set temperatures (T)

T (K)	FL = 0.0 Wt.%		FL = 0.40 Wt.%	
	s_1	σ_b (S m ⁻¹)	s_1	σ_b (S m ⁻¹)
303	0.592	3.45×10^{-8}	0.360	4.39×10^{-6}
313	0.322	8.20×10^{-8}	0.270	9.01×10^{-6}
323	0.261	1.23×10^{-7}	0.258	2.66×10^{-5}
333	0.230	2.51×10^{-7}	0.210	5.59×10^{-5}
343	0.211	5.93×10^{-7}	0.197	7.52×10^{-5}
353	0.196	9.74×10^{-7}	0.183	1.12×10^{-4}

the side chains of polymer chain) in presence of the applied AC field, and this causes an increase in conductivity. In the case of 0.40 Wt % titania filled PAM, apart from the rotation of functional groups, the increase in conductivity is due to the titania NPs added into the PAM matrix, which increases the

flexibility of polymer chains by the formation of complexes (due to the interaction of titania NPs with PAM), thereby reducing the barrier height between the trapping sites. Due to the formation of CTCs, a conducting path is created through the amorphous regions of the polymer matrix, which enhances the electrical conductivity of the composite material²⁷. The number of CTCs formed increases with the increased incorporation of TiO₂ in PAM, and this will enhance the mobility of charge carriers during polarization. The presence of CTCs results in a reduction of the crystalline-amorphous interfaces, due to which the inter - facial barrier will decrease and the electron hopping across the barrier comprising of insulator chains will increase. This will provide conductive pathways in the polymer matrix by transferring of charges from one CTC to the other^{28,29}. But, further incorporation of TiO₂ NPs into the polymer matrix leads to aggregation of the filler, which results in partial blockage of conductive paths³⁰.

The frequency dependent total conductivity of PAM and TiO₂ NP filled PAM composite films obeys Jonscher's 'universal power law' behavior³¹. According to this law, the total frequency dependent conductivity has contributions from both the AC and DC components, as given by the following relation; see equation (17).

$$\sigma(\omega) = \sigma_{DC} + \sigma_{AC} \quad \dots (17)$$

$$\sigma_{AC}(\omega) = A\omega^s \quad \dots (18)$$

$$\sigma(\omega) = \sigma_{DC} + A\omega^s \quad \dots (19)$$

In equation (18) and equation (19), the pre-exponential factor, A, is independent of frequency, but is dependent on the sample temperature³², $\omega = 2\pi f$ is the angular frequency and s is a temperature dependent frequency exponent; $0 < s < 1$.

The plot of $\log \sigma$ versus $\log f$ can be separated into two regions. In the lower frequency region, the increase in σ with respect to frequency is very less. This region is characterized by low ionic conductivity, due to the accumulation of charge carriers at the interface, which restricts the mobility of charge carriers, and thus exhibits a frequency independent nature. The conductivity in lower frequency region corresponds to DC conductivity (σ_{DC}). The higher frequency region is frequency dependent, wherein the conductivity is due to ion migration (on application of the AC signal). The slope of the straight line fit in the plot of $\log \sigma$ versus $\log f$ in the higher frequency region is used to calculate the

value of s , and the same is tabulated in Fig. 6; it is designated as ' s_1 '. The increase in conductivity of the sample with respect to change in its temperature is due to the increased vibrational motion of atoms present in the polymeric chains of the host material.

4 Conclusions

Solution casting technique was employed to obtain free standing composite samples of TiO₂ NP filled PAM, with FLs ranging from 0.02 Wt% up to 19.5 Wt%. SEM images revealed good dispersion of titania NPs in the polymeric (PAM) host material at low FLs (FL = 0.02 and 0.4 Wt%). The TiO₂ NP filled PAM composite with FLs varying from 0.02 up to 1.1Wt % exhibited improved electrical properties. A maximum decrease in the activation energy was observed for composite sample with FL equal to 0.40 Wt% when compared to pure PAM. This may be attributed to the better dispersion of NPs in the polymeric host at these lower FLs. An increase in E_a was observed due to the aggregation of the filler. DC electrical measurements revealed a decrease in activation energy for thermally stimulated mobility of charge carriers, and so the electrical conductivity increases at low FLs. Wagner's polarization technique was used to determine the nature of mobile charge carriers responsible for electrical conductivity of the titania NP filled PAM composite samples, and the study revealed that majority of these charge carriers were ions. The dielectric properties of TiO₂ NP filled PAM composite films which have been prepared by using a simple solution casting technique were examined over a wide range of frequencies (from 12Hz up to 200kHz) and temperatures (from 303K up to 353K). The results revealed that the composite sample with FL equal to 0.40 Wt % exhibits maximum enhancement in the values of dielectric constant and bulk conductivity. The enhancement of dielectric parameters with increase in temperature revealed that the conduction process was thermally activated. The enhancement in the conductivity of the TiO₂ filled PAM composite samples is due to increase in the movement of hopping charge carriers. The incorporation of TiO₂ NPs in the PAM matrix creates new conducting paths for the movement of charge carriers.

Acknowledgements

The authors acknowledge that the XRD scans and SEM images were recorded at Manipal Institute of Technology (MIT), Manipal and Indian Institute of

Technology (IIT), Kanpur, respectively. One of the authors (G Veena) acknowledges the receipt of RGNF fellowship from the University Grants Commission (UGC), Government of India.

References

- 1 Shameem M M, Sasikanth S M, Annamalai R & Raman R G, *Mater Today Proc*, 45 (2021) 2536.
- 2 Hassan T, Salam A, Khan A, Khan S U, Khanzada H, X Wasim M, Khan M Q & Kim I S, *Functional J Polym Res*, 28 (2021) 36.
- 3 Dhatarwal P & Sengwa R J, *Physica B: Condensed Matter*, 613 (2021) 412989.
- 4 Taha T A & Alzara M A A, *J Mol Struct*, 1238 (2021) 130401.
- 5 Jamatia T, Skoda D, Urbanek P, Sevcik J, Maslik J, Munster L, Kalina L & Kuritka I, *J Mater Sci Mater Electron*, 30 (2019) 11269.
- 6 Seo J, Cho M J, Cartwright A N & Prasad P N, *Adv Mater*, 23 (2011) 3984.
- 7 Lai C, Low W F W, Siddick S Z B M & Juan J C, Chapter 12 :*Graphene/TiO₂ Nanocomposites: Synthesis Routes, Characterization, and Solar Cell Applications*, in: *Handbook of graphene set, I-VIII*, (Eds: Celasco E, Chaika A N, *et al*), (John Wiley and Sons), 2019.
- 8 Oh J, Fabrication of ruthenium / conducting polymer hybrid nanoparticle and its application as hydrogen chemical sensor Ph.D Thesis, Seoul National University, South Korea, 2019.
- 9 Huang Z, Guo H & Zhang C, *Compos Commun* 12 (2019) 117.
- 10 Jagadeesan A, Sasikumar M, Jeevani R, Therese H A, Ananth N & Sivakumar P, *J Mater Sci Mater Electron*, 30 (2019) 17181.
- 11 Huyen D N, Tung N T, Thien N D & Thanh L H, *Sensors*, 11 (2011) 1924.
- 12 Idris N H M, Rajakumar J, Cheong K Y, Kennedy B J, Ohno T, Yamakata A & Lee H L, *ACS Omega*, 6 (2021) 14493.
- 13 Singh P K, Bhattacharya B & Nagarale R K, *J Appl Polym Sci*, 118 (2010) 2976.
- 14 Miao H, Chen B, Li S, Wu X, Wang Q, Zhang C, Sun Z & Li H, *J Power Sources*, 450 (2020) 227653.
- 15 Abutalib M M & Rajeh A, *Physica B: Condensed Matter*, 578 (2020) 411796.
- 16 Gaabour L H, *J Mater Res Technol*, 8 (2019) 2157.
- 17 Pal M, García-Serrano J, Santiago P & Pal U, *J Phys Chem C*, 111 (2007) 96.
- 18 Li G, Li L, Boerio-Goates J & Woodfield B F, *J Am Chem Soc*, 127 (2005) 8659.
- 19 Olad A, Behboudi S & Entezami A A, *Bull Mater Sci*, 35 (2012) 801.
- 20 Baraker B M & Lobo B, *Canadian J Phys*, 95 (2017) 738.
- 21 Vishwas M, Narasimha Rao K, Neela Priya D, Raichur A M, Chakradhar R P S & Venkateswarlu K, *Proc Mater Sci*, 5 (2014) 847854.
- 22 Theivasanthi T & Alagar M, Titanium dioxide (TiO₂) nanoparticles—XRD analysis: An insight, preprint. arXiv:1307.1091
- 23 Agrawal R C, *Indian J Pure Appl Phys*, 37 (1999) 294.
- 24 Wagner J B & Wagner C, *J Chem Phys*, 26 (1957) 1597.
- 25 Xu W, Siow K S, Gao Z & Lee S Y, *J Electrochem Soc*, 146 (1999) 4410.
- 26 Nadimicherla R, Sharma A K, Narasimha Rao V V R & Chen W, *Measurement*, 47 (2014) 33.
- 27 Hdidar M, Chouikhi S, Fattoum A, Arous M & Kallel A, *J Alloys Compd*, 750 (2018) 375.
- 28 Su S & Kuramoto N, *Synth Metal J*, 114 (2000) 147.
- 29 Srivastava S, Kumar S, Singh V N, Singh M & Vijay Y K, *Int J Hydrog Energy*, 36 (2011) 6343.
- 30 Rao V, Ashokan P V & Shridhar M H, *Mater Sci Eng A*, 281 (2000) 213.
- 31 Jonscher A K, *Nature*, 267 (1977) 673.
- 32 Gogulamurali N, Suthanthiraraj S A & Maruthamuthu P, *Solid State Ionics*, 86 (1996) 1403.